Genome Scale Reconstruction of a *Salmonella* Metabolic Model
COMPARISON OF SIMILARITY AND DIFFERENCES WITH A COMMENSAL ESCHERICHIA COLI STRAIN*[S]

Manal AbuOun[‡1,2], **Patrick F. Suthers**[§1], **Gareth I. Jones**[‡], **Ben R. Carter**[¶], **Mark P. Saunders**[‡], **Costas D. Maranas**[§], **Martin J. Woodward**[‡], **and Muna F. Anjum**[‡]

From the [‡]Department of Food and Environmental Safety, Veterinary Laboratories Agency (Weybridge), Addlestone, Surrey KT15 3NB, United Kingdom, [§]Pennsylvania State University, University Park, Pennsylvania 16802, and [¶]South East Wales Trials Unit, School of Medicine, Cardiff University, Cardiff CF14 4XN, Wales, United Kingdom

Salmonella are closely related to commensal *Escherichia coli* but have gained virulence factors enabling them to behave as enteric pathogens. Less well studied are the similarities and differences that exist between the metabolic properties of these organisms that may contribute toward niche adaptation of *Salmonella* pathogens. To address this, we have constructed a genome scale *Salmonella* metabolic model (*i*MA945). The model comprises 945 open reading frames or genes, 1964 reactions, and 1036 metabolites. There was significant overlap with genes present in *E. coli* MG1655 model *i*AF1260. *In silico* growth predictions were simulated using the model on different carbon, nitrogen, phosphorous, and sulfur sources. These were compared with substrate utilization data gathered from high throughput phenotyping microarrays revealing good agreement. Of the compounds tested, the majority were utilizable by both *Salmonella* and *E. coli*. Nevertheless a number of differences were identified both between *Salmonella* and *E. coli* and also within the *Salmonella* strains included. These differences provide valuable insight into differences between a commensal and a closely related pathogen and within different pathogenic strains opening new avenues for future explorations.

Salmonella is a major cause of human and animal enteric disease. *Salmonella* consists of two species, *bongori* and *enterica*, and the latter can be further divided into subspecies (I-VI). The majority of human and animal infections are caused by *S. enterica* subspecies I, of which *Salmonella typhimurium* and *Salmonella enteritidis* are the most prevalent causes of human inflammatory gastroenteritis, often referred to as food poisoning (1). The recent availability of genome sequences of bacterial pathogens, including *Salmonella*, provides an opportunity to interrogate these organisms using a systems biology approach. By contrasting the genotype-phenotype relationship of pathogens such as *Salmonella* against closely related commensals such as an *Escherichia coli* K12 insights can be revealed

into how these pathogens have adapted to their environmental niche(s). *Salmonella* and *E. coli* K12 share ~85% of their genome (2–6). DNA microarray and genome sequencing studies have highlighted regions of the genome that are conserved between these closely related bacteria and those that are different. Many of the differences are attributable to the acquisition of virulence factors, although a significant proportion of their genome codes is for metabolic genes (2–8).

A genome scale model consists of a stoichiometric reconstruction of all reactions known to act in the metabolism of an organism along with a set of accompanying constraints on the flux of each reaction in the system (9, 10). These models define the organism's global metabolic space, network structural properties, and flux distribution potential (9, 10). Therefore constraint-based models can help predict cellular phenotypes given particular environmental conditions. Genome scale models have been useful in understanding the metabolic properties of a variety of organisms including *E. coli*, *Bacillus subtilis*, *Pseudomonas putida*, and *Lactobacillus* (9–12). Genome scale models can be validated in various ways such as continuous culture experiments, substrate utilization assays, specific gene mutations, and isotopic carbon measurements. The high through-put phenotype microarray (PM)[3] system that is available through Biolog (Hayward, CA) is ideal to use for substrate utilization assays as it provides a comprehensive large-scale phenotyping technology to assess gene function at the cellular level (13).

The aim of this work was to construct a *Salmonella* genome scale model. The model highlights the similarities and differences between pathogenic bacteria such as *S. typhimurium* and *S. enteritidis* and the commensal *E. coli* K12 laboratory strains. The model was validated using the PM system and literature-derived (*i.e.* bibliomic) information. The substrate utilization assays also highlighted current knowledge gaps that will require further experimental data that can be used in the future for refining and extending the model.

EXPERIMENTAL PROCEDURES

Phenotype MicroArray (Biolog)—*E. coli* MG1655 was obtained from ATCC (700926), *S. typhimurium* LT2 (ACTCC 700220),

[3] The abbreviations used are: PM, phenotype microarray; COGs, Cluster of Orthologous Genes; DT, definitive type; PT, phage type; 4-HPA, hydroxyl-phenylacetic acid; ORF, open reading frame.

S. typhimurium DT104 (NCTC 13348), and *S. enteritidis* PT4 (NCTC 13349) were obtained from the Sanger Center (Wellcome Trust Genome Campus, Hinxton, Cambridge). The four bacterial strains were analyzed using the OmniLog Phenotype MicroArray technology provided by Biolog (13) that allows high throughput substrate utilization screening of bacterial cells and included 191 sole carbon sources, 95 sole nitrogen sources, 59 sole phosphorus sources, and 35 sole sulfur sources. All fluids, reagents and PM panels were supplied by Biolog and used according to the manufacturer's instructions. Briefly, bacterial strains were cultured for 16 h on Luria-Bertani agar plates at 37 °C. Cells were picked from the agar surface with a sterile cotton swab and suspended in 10 ml of inoculating fluid (IF-0), and the cell density was adjusted to 85% transmittance (T) on a Biolog turbidimeter. The minimal media inoculating fluid (IF-0) contained 100 mM NaCl, 30 mM triethanolamine-HCl (pH 7.1), 5.0 mM NH_4Cl, 2.0 mM NaH_2PO_4, 0.25 mMNa_2SO_4, 0.05 mM $MgCl_2$, 1.0 mM KCl, 1.0 μM ferric chloride, and 0.01% tetrazolium violet (13). Before the addition to PM microtiter plates, bacterial suspensions were further diluted into 12 ml of IF-0 (per plate) in the relevant inoculating fluid. The carbon source for PM3 and -4 experiments that measure nitrogen, phosphorus, sulfur, and peptide utilization was 20 mM sodium succinate and 2 μM ferric citrate. Substrate utilization was measured via the reduction of a tetrazolium dye forming a purple formazan (supplied by Biolog) and is indicative of active cellular respiration at 37 °C. Formazan formation was monitored at 15-min intervals for 26 h. Kinetic data were analyzed with OmniLog-PM software. Each experiment was performed at least twice per strain. The list of compounds and the ability of each strain to utilize these substrates are detailed in the supplemental files AbuOunSuppl-01 to AbuOunSuppl-04). It must be noted that although tetrazolium dye reduction is indicative of cellular respiration, it may occur independent of cell growth (cell multiplication/formation of biomass) in some cases (13, 14).

Model Construction—The *S. typhimurium* metabolic model was constructed starting with the core gene data set present in *E. coli* (7) and the annotated genome of *S. typhimurium* LT2. We then made use of the recently published *i*AF1260 metabolic model of *E. coli* MG1655 (ECO/K12) (15) to identify the reactions and to establish the gene-protein reaction associations that could be directly incorporated into the initial *Salmonella* model. Protein homology searches were used to identify additional genes and reactions to append to the model. These reactions were added to the model after evaluating charge and elemental balancing. A list of reactions, gene associations, exchange fluxes, and metabolites included in *Salmonella* model construction are detailed in supplemental file AbuOunSuppl-05.

Generation of the Biomass Equation—The biomass equation was generated by accounting for as many as possible of the constituents that form the cellular biomass of *S. typhimurium*. We started with the biomass equation from the core biomass equation from the *E. coli i*AF1260 metabolic model (15). Amino acid utilization was incorporated as charged, and uncharged

tRNA molecules in the biomass equation was incorporated as reactants and products, respectively.

Generation of a Computations-ready Model—Testing the metabolic model using optimization-based approaches requires the definition of a number of sets and parameters. Sets: I, $\{i\}$ = set of metabolites; $J = \{j\}$ = set of reactions; $J^R \subseteq J$ = set of reversible reactions; $I^E \subseteq$ metabolites that can cross cell boundaries (either direction); $I^F \subseteq I$ = metabolites present in growth medium. Parameters: S_{ij} = stoichiometric matrix; LB_j = lower bound of flux of reaction j; UB_j = upper bound of flux of reaction j. Variable: v_j = flux of reaction j; upper and lower bounds; UB_j and LB_j, were chosen as not to exclude any physiologically relevant metabolic flux values. The upper bound for all reaction fluxes was set to 1000. The lower bound was set equal to 0 for irreversible reactions and to -1000 for reversible reactions. The non-growth associated ATP maintenance limit was set to $LB_{ATPM} = 8.4$ per g of dry weight/h. The maximum transport rate into the cell was 20 mmol of per g of dry weight/h (*i.e.* $LB_j = -20$) for any source exchange reactions (15).

Using the principle of stoichiometric analysis along with the application of a pseudo-steady-state hypothesis to the intracellular metabolites (16), an overall flux balance can be written as follows.

$$\sum_j S_{ij} \cdot v_j = 0, \ \forall \ i \ \epsilon \ I \qquad \text{(Eq. 1)}$$

When constructing the model, we also generated the gene-protein reaction associations that link the ORFs to the reactions that are catalyzed by their gene products using standard conventions (17).

Analysis and Restoration of Network Connectivity—Once a mathematical representation of the metabolic model was generated, we first determined using GapFind (18) which metabolites could not be produced (*i.e.* cannot carry any net influx) given the availability of all substrates supported by the model. Much of the results obtained through GapFill (18) was subsumed by GrowMatch (19) (described briefly below), but blocked metabolites known to be present in *S. typhimurium* (*e.g.* adenosylcobalamin) were unblocked using GapFill.

Model Adjustment Using in Vivo Phenotypes—We tested the *in silico* growth predictions of the *S. typhimurium* metabolism network by examining the flux of the biomass equation. Given a particular growth environment, we solved the following formulation: maximize $v_{biomass}$, subject to Equations 1 and 2,

$$LB_j \cdot w_j \le v_j \le UB_j \cdot w_j, \ \forall \ j \ \epsilon \ J \qquad \text{(Eq. 2)}$$

We simulated a particular growth environment by setting $LB_j = -20$ for only the reactions associated with the components in the medium. This formulation was solved for each source condition using CPLEX Version 11 accessed within the General Algebraic Modelling System modeling environment to directly compare with the Biolog PM panels. During these comparisons oxygen uptake was permitted in both experiments and simulations, and the presence or absence of growth was tabulated for both experiment and model.

We next applied the GrowMatch method to reconcile inconsistencies between *in silico* and *in vivo* growth predictions (19).

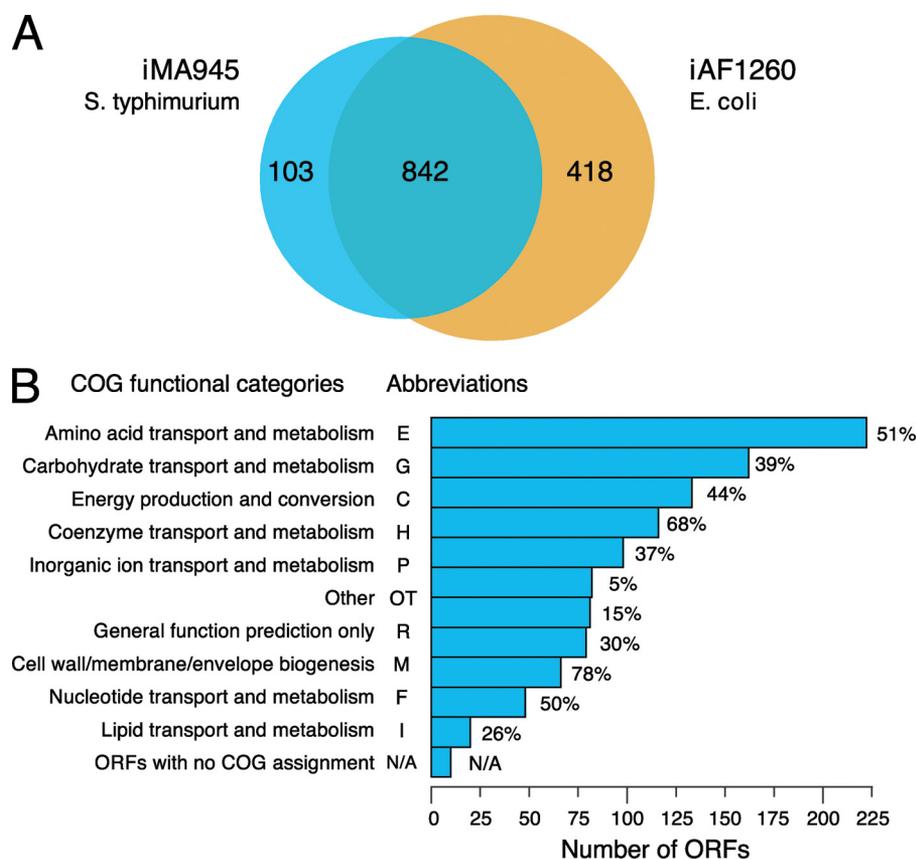# Comparison of Salmonella and E. coli Metabolic Properties

FIGURE 1. *A*, a Venn diagram that shows the homology overlap between the *S. typhimurium* model *i*MA945 and the *E. coli* model *i*AF1260. *B*, classification of the ORFs included in *i*MA945 grouped into COG functional categories. The length of each *bar* represents the number of genes in each COG that is included in the model. The percent assigned to each class refers to the coverage of the total number in the genome accounted for in the model. Some of the ORFs do not currently have a COG functional category assignment (here represented as *N/A*). Note that although each ORF is only counted once within each COG functional category, some ORFs have multiple COG category assignments.

work. As in the earlier steps of the model generation, the addition of reactions was carefully monitored, and we associated ORFs with these reactions where possible.

RESULTS

Reconstruction of Metabolic Network—The general principles of the metabolic reconstruction process have been previously outlined (15, 22). We followed a recently published reconstruction process that makes use of semiautomated tools during the series of successive refinements (23). Briefly, this process involves 1) identification of biotransformations using homology searches, 2) assembly of reaction sets into a genome scale metabolic model, 3) network connectivity analysis and restoration, and 4) evaluation and improvement of model performance when compared with *in vivo* growth phenotypes; details are available in the supplemental Excel file AbuOunSuppl-06.

During the first step, the *S. typhimurium* metabolic model was initially constructed using the core gene data set also present in *E. coli* genes (7) and the annotated genome of LT2 (5). We then used these homologies to generate a list of those genes present in the current *E. coli* metabolic reconstruction *i*AF1260 model (15). We used *i*AF1260 to identify the reactions and to establish the gene-protein reaction associations that could be directly incorporated into the initial *Salmonella* model. We also added all non-gene associated reactions from *i*AF1260 that were required for aerobic growth on glucose. Homology searches from protein databases and use of the KEGG (20) and MetaCyc (21) databases were also used to identify additional genes and reactions present in *S. typhimurium*. The model was tested using optimization based approaches, and gene-protein reaction associations that link the ORFs to the reactions that are catalyzed by their gene products were also generated. GapFind and GapFill (18) were used to unblock in the model metabolites known to be present in *S. typhimurium* (see "Experimental Procedures").

Comparison of the homologous genes in *Salmonella* with those present in *i*AF1260 identified 842 ORFs that could be directly incorporated into the *Salmonella* model. A breakdown of the predicted functionality of the ORFs using COGs (Cluster of Orthologous Genes (24)) showed that the classes most represented were involved with transport and metabolism of various compounds such as amino acid, carbohydrate, lipid, and nucleotide, although genes involved in cell wall, envelope, or membrane biogenesis and energy production and conversion

Full details of the method are given in the referenced work, but the salient points of method are briefly described here. To this end, we first classified growth predictions as "Grow" for those with $v_{\text{biomass}}^{\text{max}}$ greater than zero and "NoGrow" otherwise. We then sorted growth prediction inconsistencies with the *in vivo* data into two categories; (*a*) Grow/NoGrow, Grow/NoGrow if the *in silico* model predicts growth, whereas there is no observed growth *in vivo* and (*b*) No Grow/Grow, if the *in silico* model predicts no growth in contrast with observed *in vivo* growth. In Grow/NoGrow mutants, the model over-predicts the metabolic capabilities of the organism. GrowMatch automatically restores consistency in these cases by suppressing reaction activities to prevent *in silico* growth (*i.e.* by identifying erroneously added reactions or missing regulation). Conversely, in No Grow/Grow cases, the model under-predicts the metabolic capabilities of the organism. GrowMatch restores consistency in these mutants by adding functionalities that ensure *in silico* growth consistent with *in vivo* data. The reaction source databases used by GrowMatch in this work were the KEGG (20) and MetaCyc (21) databases. In all cases, GrowMatch operates so as not to perturb any correct growth predictions. Although the focus in (19) was on gene essentiality using a single growth medium, the GrowMatch procedure is directly applicable to other growth phenotypes as used in the present

were also present (Fig. 1). Therefore, after the reconstruction process, model *i*MA945 incorporated 945 ORFs, of which 103 were unique to *Salmonella*. This could be further broken down into proteins, protein complexes, and isoenzymes. The model incorporated 1964 reactions and 1036 metabolites, which again were subdivided into various classes (see Table 1, model details are provided in supplemental file AbuOunSuppl-05).

Validation of iMA945 Using Substrate Utilization Patterns— The OmniLog PM technology system (Biolog) was used to validate the model whereby utilization of 191 carbon sources, 95 nitrogen sources, 59 phosphorus sources, and 35 sulfur sources were compared with simulations of *i*MA945 grown *in silico* in minimal medium with the respective compounds as the sole carbon, nitrogen, phosphorus, and sulfur sources (Table 2 and supplemental file AbuOunSuppl-06). For example, nitrogen source utilization was determined in the presence of sodium succinate/ferric citrate as the carbon source, sodium dihydrogen phosphate as the phosphorous source, and sodium sulfate as the sulfur source. In the case of phosphorus source utilization, sodium succinate/ferric citrate, ammonium chloride, and sodium sulfate were included as sources of carbon, nitrogen, and sulfur, respectively. *In silico* growth yields were calculated using the biomass composition and growth-associated and non-growth-associated energy maintenance factors taken from the *E. coli* model (15).

The model was able to predict growth with 147 of the 191 carbon, 83 of the 95 nitrogen, 41 of the 59 phosphorous, and 18 of the 35 sulfur compounds correctly. In general, the total accuracy, sensitivity, and specificity were well above the standards established for metabolic genome reconstructions (see Table

2). In fact, a comparison of the *i*MA945 model with *in silico* and substrate utilization data from *i*AF1260 (15) reveals higher percentage total accuracy and specificity for carbon and nitrogen growth in *i*MA945, although they were similar for phosphorus and sulfur. For examples, comparison of predicted growth yields using the *in silico* predictions show compounds such as D-malic acid as a carbon source or L-tryptophan as a nitrogen source results in no growth for *Salmonella*, whereas maltose as a carbon source or adenosine as nitrogen source provides adequate *in silico* growth yields (see the supplemental data). The PM data match these predictions (see supplemental data). These results indicate that even though *E. coli* biomass composition was taken to predict *in silico* growth yields because of a lack of *Salmonella*-specific experimental information, the resulting predictions were congruous with *in vivo* experiments. However, in the future the model should be validated with *Salmonella*-specific biomass composition to evaluate the "true" energy cost to the living and growing *Salmonella* cells using different substrates.

Metabolic Differences between Salmonella and E. coli K12 and within Salmonella Strains—Both the model and the PM data helped us to identify metabolic differences between *Salmonella* and *E. coli* K12. Of the 379 conditions tested there were only 19 conditions under which *E. coli* K12 was unable to utilize substrates that *Salmonella* were able to utilize and 17 conditions in which *E. coli* K12 was able to utilize substrates that all three *Salmonella* strains included in our study were unable to utilize. These results allude to a common evolutionary pathway by which these enteric bacteria have evolved, and the fact that *Salmonella* and *E. coli* share ~85% of their genomes (7, 25) is also reflected in conservation of many of their metabolic properties. For the majority of differences seen in substrate utilization between the two organisms we were able to assign corresponding genes and explanations (Table 3). The most common factor was due to the presence of operons or genes in *Salmonella* that were absent from *E. coli* and vice versa. Examples of genes/operons that are present in *Salmonella* but are absent from *E. coli* K12 include the *apeE* gene, *pdu* operon, *rtl* gene, and the *hpa* operon that confer the ability for *Salmonella* to utilize Tween 40 or 80, 1–2-propanediol, adonitol/ribitol, and *p*-hydroxyphenylacetic acid, respectively. Genomic regions/ genes that are present in *E. coli* but absent in *Salmonella* included *ebgAC* genes, *als* operon, and *tnaAB*, which confer the ability for *E. coli* to utilize lactulose, β-D-allose, and L-tryptophan, respectively (Table 3). There were several instances

TABLE 1
Properties of *Salmonella i*MA945 model

Included genes	945
Proteins	810
Protein complexes	129
Isozymes	233
Reactions	1964
Metabolic reactions	1267
Transport reactions	697
Gene-protein reaction associations	
Gene-associated (metabolic transport)	1722
Spontaneous	29
Non-gene-associated (metabolic transport)	213
Exchange reactions	335
Metabolites	1036
Cytoplasmic	937
Periplasmic	445
Extracellular	330

TABLE 2
Validation of *i*MA945 metabolic model using substrate assays

E, experimental; C, computational; G, growth; NG, no growth; T, true; F, false; P, positive; N, negative; NAN, not a number (division by zero). Accuracy = (TP + TN)/(TP + TN + FP + FN); sensitivity = TP/(TP + FN); specificity = TN/(TN + FP).

Source	Substrates	Overall agreement	Compounds with exchange reactions	Agreement		Total accuracy	Disagreement		Sensitivity	Specificity
				E-G C-G TP	E-NG C-NG TN		E-NG C-G FP	E-G C-NG FN		
						%			%	%
Carbon	191	147	92	65	14	85.9	12	1	98.5	53.8
Nitrogen	95	83	66	35	20	83.3	7	4	89.7	74.1
Phosphorous	59	41	29	28	0	96.6	0	1	96.6	NAN
Sulfur	35	18	14	5	4	64.3	0	5	50.0	100.0
Total	380	289	201	133	38	85.1	19	11	92.4	66.7

Comparison of Salmonella and E. coli Metabolic Properties

TABLE 3

Metabolic differences between E. coli and Salmonella

Phenotypic differences were compared with the predicted growth, and where possible a plausible explanation has been given for these differences. E, experimental; C, computational.

Source	Compound	Model abbreviation	E. coli MG1655 (E)[a]	E. coli MG1655 (C)[a]	Salmonella (E)[a,b]	Salmonella (C)[a,b]	Gene/mutation	Explanation
Carbon	L-Proline	EX_pro-L	0	1	1	1	glnP	Mutation in glnP, the glutamine-binding protein, results in the inability to grow on proline (29)
Carbon	L-Glutamic acid	EX_glu-L	0	1	1	1	glnP	Mutation in glnP results in an inability to grow on L-glutamate (29)
Carbon	Dulcitol/galactitol	EX_galt	0	1	1	1	kba	Many E. coli K12 strains harbor a thermolabile-specific aldolase involved in galactitol degradation (51)
Carbon	L-Asparagine	EX_asn-L	0	1	1	1	ansB	FNR i.e. anaerobiosis-dependent expression of ansB (L-asparagine II) occurs in E. coli but not Salmonella (37)
Carbon	D-Glucosaminic acid		0		1		–	–
Carbon	1,2-Propanediol	EX_12ppd-S	0	1	1	1	pduCDEGHPQW	The pdu operon is present in Salmonella but absent in E. coli (38, 52)
Carbon	Tween 40		0	–	1	–	apeE	ApeE, an outer membrane esterase present in Salmonella, allows hydrolysis of naphthyl esters (53, 54)
Carbon	Tween 80		0	–	1	–	apeE	ApeE, an outer membrane esterase present in Salmonella, allows hydrolysis of naphthyl esters (53, 54)
Carbon	Adonitol/ribitol		0	–	1	–	rtlBAC	Genes for ribitol catabolism missing in E. coli K12 (55, 56)
Carbon	Citric acid	EX_cit	0	1	1	1	citAB (tcuABC)	The cit/tcu operon is absent in most E. coli but enables citrate utilization in Salmonella (57)
Carbon	Tricarballylic acid		0	–	1	–	citAB (tcuABC)	The cit/tcu operon, absent in E. coli, is also responsible for metabolism of the structurally related tricarballylic acid (58)
Carbon	p-Hydroxy phenyl acetic cid	EX_4hphac	0	–	1	1	hpaBC, hpaGEDFHI, hpaR, hpaA, and hpaX	The hpa operon required for catabolism of 4-HPA is present in Salmonella but missing in E. coli K12 strains (39)
Carbon	m-Hydroxy phenyl acetic acid		0	–	1	–	hpaBC, hpaGEDFHI, hpaR, hpaA, and hpaX	The hpa operon required for catabolism of 4-HPA is present in Salmonella but missing in E. coli K12 (39)
Carbon	D-Psicose		0	–	1	–	–	–
Carbon	2-Deoxy-D-ribose		0	–	1	–	deoQKPX	The deoQKPX operon, absent from E. coli, is required for the uptake, phosphorylation, and regulation of 2-deoxy-D-ribose utilization (59)
Carbon	D-Tagatose		0	–	1	–	tagKHT	The presence of tag genes in the gat (galactitol) operon enables degradation of D-tagatose in Salmonella
Carbon	D-Tartaric acid		0	–	1	–	–	–
Carbon	Tyramine	EX_tym	0	0	1	1	hpa operon	In Salmonella, tyramine utilization as a carbon source results from its oxidative deamination by the cell membrane-bound tyramine oxidase (TynA/MaoA) to 4-HPA, requiring the hpa operon, which is absent from E. coli K12 (60)
Carbon	Lactulose		1	–	0	–	ebgAC	The ebg operon required for lactulose utilization is absent in Salmonella (61, 62)
Carbon	D-Malic acid	EX_mal-D	1	1	0	0	yeaUI/ttuC	Tartrate dehydrogenase, yeaUI or ttuC, required for the breakdown of D-malate, is present in E. coli (22, 63) but absent from Salmonella

TABLE 3—continued

Source	Compound	Model abbreviation	E. coli MG1655 (E)[a]	E. coli MG1655 (C)[a]	Salmonella (E)[a,b]	Salmonella (C)[a,b]	Gene/mutation	Explanation
Carbon	L-Galactonicacid-γ-lactone	EX_galctn-L	1	1	0	1	YjjLMN	Growth dependent on the *yjj* operon (22), which is only partially present in *S. typhimurium* LT2
Carbon	D-Galacturonic acid	EX_galur	1	1	0	1	*exuT–uxaCA* and *uxaB*	Genes required for the hexauronate catabolism *exuT–uxaCA* and *uxaB* (64) are absent in *S. typhimurium*
Carbon	β-D-Allose	EX_all-D	1	1	0	0	*alsRBACEK*	The β-D-allose utilization genes found in *E. coli* (65, 66) are missing from the *Salmonella*-sequenced genomes including *S. typhimurium*
Carbon	3-0-β-D-Galactopyranosyl-D-arabinose		1	–	0	–	–	–
Carbon	β-Methyl-D-galactoside		1	–	0	–	*ebg* and *lac* systems	This is probably due to absence of the *ebg* and *lac* system in *Salmonella*
Nitrogen	Tyramine	EX_tym	0	1	1	1	*maoB*/tyramine	In *E. coli*, tyramine concentration and *maoB* regulate its utilization (31)
Nitrogen	N-Acetyl-D-mannosamine (ManNAc)	EX_acmana	0	1	1	1	*mlc* and *nanR*	Mlc and NanR regulators repress expression of the *manXYZ*-encoded transporter for ManNAc uptake and *nan* genes for its utilization, resulting in very slow growth in *E. coli* K12 (67)
Nitrogen	L-Tryptophan	EX_trp-L	1	1	0	0	*tnaAB*	The L-tryptophan inducible tryptophanase utilized by *E. coli* (68) is missing in *Salmonella*
Nitrogen	Cytosine	EX_csn	1	1	0	0	*codAB* and *nac*	*E. coli* contains the *codAB* genes required for cytosine uptake and deamination regulated by Nac (69), which are absent in *S. typhimurium*
Phosphorus	Carbamyol phosphate		1	–	0	–	*yeaI, phoA,* and *ynbD*	Three phosphatases (YeaI, PhoA, YnbD), which may enable *E. coli* to cleave phosphorous from phosphate esters, are absent in *Salmonella* (70)
Phosphorus	Phosphoryl choline		1	–	0	–	*betT*	BetT, the high affinity choline transporter present in *E. coli* (71), is absent in *S. typhimurium*, which also has the three phosphatases missing
Sulfur	Taurocholic acid		1	–	0	–	*ssuEADCB* or *tauABC tauD*	The two sulfonate systems present in *E. coli* are absent in *Salmonella* and may be responsible for utilization of this compound
Sulfur	Taurine	EX_taur	1	1	0	0	*tauABC tauD*	The taurine uptake and utilization operon from *E. coli* (72, 73) is absent in *Salmonella*
Sulfur	Hypotaurine		1	–	0	–	*tauABC tauD*	Hypotaurine is probably utilized by the same operon in *E. coli*
Sulfur	Butane sulfonic acid	EX_butso3	1	1	0	0	*ssuEADCB*	This operon is present in *E. coli* under regulation of CysB and Cbl and is required for butane sulfonic acid utilization (74–76)
Sulfur	2-Hydroxyethane sulfonic acid	EX_isetac	1	1	0	0	*ssuEADCB*	The *ssu* operon is also involved in 2-hydroxyethane sulfonic acid utilization in *E. coli*
Sulfur	Methane sulfonic acid	EX_mso3	1	1	0	0	*ssuEADCB*	The *ssu* operon is also involved in methane sulfonic acid utilization in *E. coli*

[a] 0 indicates no respiration was observed when grown in compound, 1 indicates respiration was observed when grown in compound, and – indicates that no data are available.
[b] Collated Biolog data are from *S. typhimurium* LT2, DT104 and *S. enteritidis* PT4.

where the most plausible explanation for the differences seen in substrate utilization was given, *e.g.* phosphocholine, taurocholic acid, or taurine utilization. These explanations require verification in the future by either complementing *Salmonella* strains with the respective genes or operon or by mutating the genetic pathway in *E. coli*.

Comparative genomic hybridization microarray have shown that strains from *S. enterica* subspecies I have a large portion of their genome conserved (7); therefore, it was not unexpected that of the compounds tested, only six showed differences in substrate utilization between the *Salmonella* strains. Differences included the inability to utilize L-histidine, L- and *meso*-tartaric acid, D-tagatose, glyoxylic acid, and D-saccharic acid (see the supplemental data). Interrogation of the *S. typhimurium* LT2 genome indicated that the *hutU* gene, involved in histidine metabolism (26, 27), harbored a frameshift mutation and, hence, is a pseudogene. This gene mutation is not present in *S. typhimurium* definitive type (DT) 104 or the *S. enteritidis* phage type (PT) 4 strain genome sequence (Sanger Institute), which unlike LT2, are both able to utilize histidine. *S. typhimurium* DT104 strains are missing a group of genes (STM0517-STM0529) involved in allantoin utilization (28) that is also involved in glyoxylic acid utilization.[4] Again, these genes are present in both LT2 and PT4 strains, which unlike DT104 are able to utilize this substrate. *S. enteritidis* PT4 is unable to catabolize D-tagatose probably because of the absence of the *tag* operon (*tagKHT*) responsible for D-tagatose utilization in the genome sequence of *S. enteritidis* PT4; this operon is present in the both *S. typhimurium* strains, which are able to utilize D-tagatose. PT4 was unable to utilize D-saccharic acid, whereas DT104 was unable to utilize both *levo* and *meso*-tartaric acid, and LT2 was unable to utilize L-tartaric acid. These differences were not readily explainable and will require future experimental work. Further experimental work using strains from different *Salmonella* serovars and phage types will also inform whether a large core of metabolic properties in *Salmonella* are conserved and the *Salmonella* model *i*MA945 can be adapted to different serovars and definitive or phage types by including strain specific differences such as those identified in this study. In the future conditions such as osmolarity and pH, which are important stress responses that are likely to be involved in niche specific adaptation, should also be included.

Discrepancies and Future Refinement of the Model—Several discrepancies were identified between substrate utilization and model predictions for both the *E. coli* (*i*AF1260) and *Salmonella* (*i*MA945) models (see the supplemental data; Table 2). For many of these an adequate explanation was not available from the literature (Table 3). For example, the model predicts growth of *E. coli* MG1655 on both L-proline and L-glutamic acid, but the PM data shows no substrate utilization in the presence of either compound. These data also match with Feist *et al.* (15) and could be due to recent point mutations acquired by strain MG1655 in *glnP*. GlnP is essential for glutamate and proline transport and catabolism (29) and requires further exploration in the future. Tyramine used as a nitrogen source was

another compound that showed discrepancy between substrate utilization data from both this data set and Feist *et al.* (15) and the model. The breakdown products of tyramine include ammonia, which should be utilizable as a nitrogen source in both *Salmonella* and *E. coli* (30). It has been shown for *E. coli* that both the presence of the MaoB regulator and tyramine concentration in the medium is essential for monoamine oxidase (MaoA) activity (31); hence, the inability of MG1655 to utilize tyramine may be an indication of insufficient tyramine in the PM medium used for these studies, although these factors seem not to have affected the ability of LT2 to utilize tyramine as a nitrogen source. This could indicate differences in regulation of tyramine metabolism in *E. coli* and *Salmonella*. There were several substrates for which an *in silico* pathway and, hence, the predicted growth yield was not available for either *i*AF1260 or *i*MA945 or for the strain-specific differences seen within *Salmonella*. As more information becomes available on the metabolism and regulation involved in utilization of some of the substrates highlighted here, it can be included in future iterations of the models to help in model refinement and to increase its accuracy.

DISCUSSION

Salmonella and *E. coli* are closely related bacterial species that have diverged from each other about a 100 million years ago (32). Since their divergence, *Salmonella* have become a pathogen for humans and animals, whereas *E. coli* largely remains a commensal (2, 5). The ability for *Salmonella* to survive within the host and cause disease has been attributed to the acquisition of specific virulence factors by horizontal gene transfer such as the *Salmonella* pathogenicity islands (8, 33, 34). These have been studied intensively over the past decade, and currently up to 10 genomic regions have been identified as *Salmonella* pathogenicity islands (25). However, metabolic differences that have enabled *Salmonella* to adapt to its specific niche are less well studied but may be key in understanding how this pathogen evolved. Therefore, the aim of this study was to construct a *Salmonella* genome scale metabolic model to identify similarities and differences between *E. coli* K12, which for this discussion we consider to be representative of a commensal strain, and *Salmonella*, which may give clues of its adaptability to a specific niche. There are significant differences between *E. coli* pathogenic types,[5] and perhaps similar approaches to those described here can be used to gain clues of their adaptation to specific niches too.

Genome scale models can be used to characterize metabolic resource allocation, experimentally testable predictions of cell phenotype, to elucidate metabolic network evolution scenarios and to design experiments that most effectively reveal genotype-phenotype relationships (9, 35). In this work comparison of the *Salmonella* genome scale model, based on that constructed for the *E. coli* strain MG1655 (15), revealed that ~90% of ORFs/genes included in the model overlap between the two organisms. This is similar to the ~85% gene overlap found from comparative genomic hybridization microarray data between MG1655 and *S. enterica* subspecies I (sspI) strains that comprise

---

[4] M. P. Saunders, unpublished data.

[5] J. Hobman, personal communication.

the *S. enterica* sspI core genome (7), highlighting their evolutionary similarity and synteny in their genomes. Further exploration and verification of model *i*MA945 using phenotypic data gathered using the OmniLog PM system (Biolog) revealed differences in utilization of carbon, nitrogen, phosphorous, and sulfur substrates between the three *Salmonella* strains and *E. coli*.

Our data showed more differences in the utilization of carbon compounds rather than nitrogen, sulfur, or phosphorous, which is contrary to the common understanding that the catabolic repertoire for carbohydrate utilization is largely the same in *E. coli* and *S. typhimurium* (36). However, this may be because of inclusion of a larger number of carbon compounds than nitrogen, phosphorous, and sulfur in the list of substrates tested. Carbon compounds that were only utilizable by *Salmonella* included a diverse range from amino acids to sugar alcohols to napthyl esters and aromatic compounds. How these compounds help *Salmonella* to adapt to its niche will need to be investigated. Interestingly, often genes involved in catabolism of these compounds *e.g.* L-proline and L-asparagine, were present in *E. coli* K12 (29, 37), and the *in silico* model predicted growth, but probably because of differences in regulation and gene expression, only *Salmonella* strains showed utilization of these substrates in the system used in this study. In other instances such as catabolism of 4-HPA and 1,2-propanediol, catabolic gene cassettes had been recruited by *Salmonella* or lost by *E. coli* to enable utilization of the compound (38, 39). Interestingly, it is only *E. coli* K12 strains that are unable to catabolize 4-HPA, as *E. coli* B, C, and W are able to fully or partially degrade 4-HPA (39–41), indicating that even within the *E. coli* genus there are considerable metabolic differences between the well studied K12 strains and other *E. coli* present in nature.

Similarly, differences were also found in substrate utilization of the *Salmonella* strains included in this study. The *S. typhimurium* DT104 strain included in this study differs from the *S. typhimurium* LT2 strain in that the former strain has acquired an extrachromosomal genomic island (*Salmonella* Genomic Island I) that confers a penta-antibiotic resistance phenotype on this strains (42, 43). This strain has been implicated in human epidemic outbreaks in the past decade, and the presence of penta-antibiotic resistance makes it difficult to treat infections (44). Similarly, *S. enteritidis* is highly prevalent in human infections, usually transmitted through chickens or eggs (1, 45). Data from Health Protection Agency, UK data base have recorded more than 40,000 cases of human infections over the past 10 years in the UK because of *S. enteritidis* PT4.[6] Therefore, although only a handful of differences were identified between the *Salmonella* strains, these differences may be significant in understanding how current pathogenic strains such as *S. typhimurium* DT104 and *S. enteritidis* PT4 have become highly successful in passing through the food chain and causing salmonellosis in humans in comparison to a largely laboratory-adapted *Salmonella* strain.

The developed *Salmonella* model provides a complementary resource to the recently published model by Raghunathan *et al.*

(46). The data presented offer an experimentally robust method for the analysis of differences and similarities between *Salmonella* serovars of medical and veterinary importance (1). In addition, the use of succinate as the source of carbon to analysis the *in silico* and *in vitro* metabolism of nitrogen, phosphorus, and sulfur has the advantage of utilizing a core tricarboxylic acid cycle compound rather than a three-carbon compound, which can lead to auxiliary dissimilatory pathways (47). Also presented are the contributions of phosphorus and sulfur metabolism, thus providing a holistic view of the metabolome of *Salmonella* serovars. Inclusion of these substrates is an important factor to consider in such metabolic genome reconstructions, as these compounds are essential components of amino acids involved in several chemical reactions and are structural components of the bacterial cell such as phosphorus in nucleic acids, adenosine triphosphate, and cell membrane phospholipids.

For future refinement and improvement of the *i*MA945 model we will integrate within the model other cellular processes such as regulation, transcription, translation, and DNA replication, which place direct metabolic and energy demands on the metabolic network (17). In fact, Covert and co-workers (48) show that in an unregulated *E. coli* genome scale network model 83.6% of the predictions were correct, whereas in the regulated network model 91.4% of predictions were correct. In addition, genome-wide single gene deletion data have proven useful during the construction and curation of metabolic models (19). For *E. coli*, these have been performed in glucose (49) or glycerol (50) minimal media. Such experiments for the *Salmonella* serovars/strains discussed here would provide significant data for refining *i*MA945. Moreover, performing growth studies of the mutant library on different growth substrates could provide additional discernment into differences in metabolism of the epidemic *Salmonella* serovars or strains.

REFERENCES

1. Rodrigue, D. C., Tauxe, R. V., and Rowe, B. (1990) *Epidemiol. Infect.* **105,** 21–27
2. Blattner, F. R., Plunkett, G., 3rd, Bloch, C. A., Perna, N. T., Burland, V., Riley, M., Collado-Vides, J., Glasner, J. D., Rode, C. K., Mayhew, G. F., Gregor, J., Davis, N. W., Kirkpatrick, H. A., Goeden, M. A., Rose, D. J., Mau, B., and Shao, Y. (1997) *Science* **277,** 1453–1462
3. Crosa, J. H., Brenner, D. J., Ewing, W. H., and Falkow, S. (1973) *J. Bacteriol.* **115,** 307–315
4. McClelland, M., Florea, L., Sanderson, K., Clifton, S. W., Parkhill, J., Churcher, C., Dougan, G., Wilson, R. K., and Miller, W. (2000) *Nucleic Acids Res.* **28,** 4974–4986
5. McClelland, M., Sanderson, K. E., Spieth, J., Clifton, S. W., Latreille, P., Courtney, L., Porwollik, S., Ali, J., Dante, M., Du, F., Hou, S., Layman, D., Leonard, S., Nguyen, C., Scott, K., Holmes, A., Grewal, N., Mulvaney, E., Ryan, E., Sun, H., Florea, L., Miller, W., Stoneking, T., Nhan, M., Waterston, R., and Wilson, R. K. (2001) *Nature* **413,** 852–856
6. McClelland, M., and Wilson, R. K. (1998) *Infect. Immun.* **66,** 4305–4312
7. Anjum, M. F., Marooney, C., Fookes, M., Baker, S., Dougan, G., Ivens, A., and Woodward, M. J. (2005) *Infect. Immun.* **73,** 7894–7905
8. Porwollik, S., Boyd, E. F., Choy, C., Cheng, P., Florea, L., Proctor, E., and

Comparison of Salmonella and E. coli Metabolic Properties

McClelland, M. (2004) *J. Bacteriol.* **186,** 5883–5898

9. Puchałka, J., Oberhardt, M. A., Godinho, M., Bielecka, A., Regenhardt, D., Timmis, K. N., Papin, J. A., and Martins dos Santos, V. A. (2008) *PLoS Comput Biol.* **4,** e1000210

10. Reed, J. L., Patel, T. R., Chen, K. H., Joyce, A. R., Applebee, M. K., Herring, C. D., Bui, O. T., Knight, E. M., Fong, S. S., and Palsson, B. O. (2006) *Proc. Natl. Acad. Sci. U.S.A.* **103,** 17480–17484

11. Ohl, M. E., and Miller, S. I. (2001) *Annu Rev. Med.* **52,** 259–274

12. Teusink, B., and Smid, E. J. (2006) *Nat. Rev. Microbiol.* **4,** 46–56

13. Bochner, B. R., Gadzinski, P., and Panomitros, E. (2001) *Genome Res.* **11,** 1246–1255

14. Bochner, B. R. (2009) *FEMS Microbiol. Rev.* **33,** 191–205

15. Feist, A. M., Henry, C. S., Reed, J. L., Krummenacker, M., Joyce, A. R., Karp, P. D., Broadbelt, L. J., Hatzimanikatis, V., and Palsson, B. Ø. (2007) *Mol. Syst. Biol.* **3,** 121

16. Vallino, J. J., and Stephanopoulos, G. (1993) *Biotechnol. Bioeng.* **41,** 633–646

17. Reed, J. L., Vo, T. D., Schilling, C. H., and Palsson, B. O. (2003) *Genome Biol.* **4,** R54

18. Satish Kumar, V., Dasika, M. S., and Maranas, C. D. (2007) *BMC Bioinformatics* **8,** 212

19. Kumar, V. S., and Maranas, C. D. (2009) *PLoS Comput. Biol.* **5,** e1000308

20. Kanehisa, M., Araki, M., Goto, S., Hattori, M., Hirakawa, M., Itoh, M., Katayama, T., Kawashima, S., Okuda, S., Tokimatsu, T., and Yamanishi, Y. (2008) *Nucleic Acids Res.* **36,** D480–D484

21. Caspi, R., Foerster, H., Fulcher, C. A., Kaipa, P., Krummenacker, M., Latendresse, M., Paley, S., Rhee, S. Y., Shearer, A. G., Tissier, C., Walk, T. C., Zhang, P., and Karp, P. D. (2008) *Nucleic Acids Res.* **36,** D623–D631

22. Reed, J. L., Famili, I., Thiele, I., and Palsson, B. O. (2006) *Nat. Rev. Genet* **7,** 130–141

23. Suthers, P. F., Dasika, M. S., Kumar, V. S., Denisov, G., Glass, J. I., and Maranas, C. D. (2009) *PLoS Comput Biol.* **5,** e1000285

24. Tatusov, R. L., Fedorova, N. D., Jackson, J. D., Jacobs, A. R., Kiryutin, B., Koonin, E. V., Krylov, D. M., Mazumder, R., Mekhedov, S. L., Nikolskaya, A. N., Rao, B. S., Smirnov, S., Sverdlov, A. V., Vasudevan, S., Wolf, Y. I., Yin, J. J., and Natale, D. A. (2003) *BMC Bioinformatics* **4,** 41

25. Parkhill, J., Dougan, G., James, K. D., Thomson, N. R., Pickard, D., Wain, J., Churcher, C., Mungall, K. L., Bentley, S. D., Holden, M. T., Sebaihia, M., Baker, S., Basham, D., Brooks, K., Chillingworth, T., Connerton, P., Cronin, A., Davis, P., Davies, R. M., Dowd, L., White, N., Farrar, J., Feltwell, T., Hamlin, N., Haque, A., Hien, T. T., Holroyd, S., Jagels, K., Krogh, A., Larsen, T. S., Leather, S., Moule, S., O'Gaora, P., Parry, C., Quail, M., Rutherford, K., Simmonds, M., Skelton, J., Stevens, K., Whitehead, S., and Barrell, B. G. (2001) *Nature* **413,** 848–852

26. Meiss, H. K., Brill, W. J., and Magasanik, B. (1969) *J. Biol. Chem.* **244,** 5382–5391

27. Smith, G. R., Halpern, Y. S., and Magasanik, B. (1971) *J. Biol. Chem.* **246,** 3320–3329

28. Matiasovicova, J., Adams, P., Barrow, P. A., Hradecka, H., Malcova, M., Karpiskova, R., Budinska, E., Pilousova, L., and Rychlik, I. (2007) *Arch. Microbiol.* **187,** 415–424

29. Masters, P. S., and Hong, J. S. (1981) *J. Bacteriol.* **147,** 805–819

30. Díaz, E., Ferrández, A., Prieto, M. A., and García, J. L. (2001) *Microbiol. Mol. Biol. Rev.* **65,** 523–569

31. Yamashita, M., Azakami, H., Yokoro, N., Roh, J. H., Suzuki, H., Kumagai, H., and Murooka, Y. (1996) *J. Bacteriol.* **178,** 2941–2947

32. Doolittle, R. F., Feng, D. F., Tsang, S., Cho, G., and Little, E. (1996) *Science* **271,** 470–477

33. Chan, K., Baker, S., Kim, C. C., Detweiler, C. S., Dougan, G., and Falkow, S. (2003) *J. Bacteriol.* **185,** 553–563

34. Ochman, H., Lawrence, J. G., and Groisman, E. A. (2000) *Nature* **405,** 299–304

35. Feist, A. M., and Palsson, B. Ø. (2008) *Nat. Biotechnol.* **26,** 659–667

36. Mayer, C., and Boos, W. (2005) *Hexose/Pentose and Hexitol/Pentitol Metabolism.* (Bock, A., ed) www.ecosal.org, American Society for Microbiology, Washington, D. C.

37. Jennings, M. P., Scott, S. P., and Beacham, I. R. (1993) *Mol. Microbiol.* **9,** 165–172

38. Price-Carter, M., Tingey, J., Bobik, T. A., and Roth, J. R. (2001) *J. Bacteriol.* **183,** 2463–2475

39. Prieto, M. A., Díaz, E., and García, J. L. (1996) *J. Bacteriol.* **178,** 111–120

40. Burlingame, R. P. (1983) *The Degradation of 3-Phenylpropionic Acid by Escherichia coli.* Ph.D. thesis, University of Minnesota

41. Cooper, R. A., and Skinner, M. A. (1980) *J. Bacteriol.* **143,** 302–306

42. Boyd, D., Peters, G. A., Cloeckaert, A., Boumedine, K. S., Chaslus-Dancla, E., Imberechts, H., and Mulvey, M. R. (2001) *J. Bacteriol.* **183,** 5725–5732

43. Doublet, B., Boyd, D., Mulvey, M. R., and Cloeckaert, A. (2005) *Mol. Microbiol.* **55,** 1911–1924

44. Threlfall, E. J., Ward, L. R., and Rowe, B. (1997) *Euro. Surveill.* **2,** 81–84

45. Humphrey, T. J., Baskerville, A., Chart, H., Rowe, B., and Whitehead, A. (1992) *Vet. Rec.* **131,** 386–388

46. Raghunathan, A., Reed, J., Shin, S., Palsson, B., and Daefler, S. (2009) *BMC Syst. Biol.* **3,** 38

47. Unden, G., and Kleefeld, A. (2004) in *Aerobic and Anaerobic Growth* (Bock, A., ed) Chapter 3.4.1., www.ecosal.org, American Society for Microbiology, Washington, D. C.

48. Covert, M. W., Knight, E. M., Reed, J. L., Herrgard, M. J., and Palsson, B. O. (2004) *Nature* **429,** 92–96

49. Baba, T., Ara, T., Hasegawa, M., Takai, Y., Okumura, Y., Baba, M., Datsenko, K. A., Tomita, M., Wanner, B. L., and Mori, H. (2006) *Mol. Syst. Biol.* **2,** 2006.0008

50. Joyce, A. R., Reed, J. L., White, A., Edwards, R., Osterman, A., Baba, T., Mori, H., Lesely, S. A., Palsson, B. Ø., and Agarwalla, S. (2006) *J. Bacteriol.* **188,** 8259–8271

51. Lin, E. C. (1996) in *Escherichia coli and Salmonella: Cellular and Molecular Biology* (Neidhardt, F. C., ed), 2nd Ed. pp. 307–342, American Society for Microbiology, Washington, D. C.

52. Chen, P., Andersson, D. I., and Roth, J. R. (1994) *J. Bacteriol.* **176,** 5474–5482

53. Carinato, M. E., Collin-Osdoby, P., Yang, X., Knox, T. M., Conlin, C. A., and Miller, C. G. (1998) *J. Bacteriol.* **180,** 3517–3521

54. Collin-Osdoby, P., and Miller, C. G. (1994) *Mol. Gen. Genet.* **243,** 674–680

55. Link, C. D., and Reiner, A. M. (1983) *Mol. Gen. Genet.* **189,** 337–339

56. Woodward, M. J., and Charles, H. P. (1983) *J. Gen. Microbiol.* **129,** 75–84

57. Reynolds, C. H., and Silver, S. (1983) *J. Bacteriol.* **156,** 1019–1024

58. Lewis, J. A., Horswill, A. R., Schwem, B. E., and Escalante-Semerena, J. C. (2004) *J. Bacteriol.* **186,** 1629–1637

59. Christensen, M., Borza, T., Dandanell, G., Gilles, A. M., Barzu, O., Kelln, R. A., and Neuhard, J. (2003) *J. Bacteriol.* **185,** 6042–6050

60. Parrott, S., Jones, S., and Cooper, R. A. (1987) *J. Gen. Microbiol.* **133,** 347–351

61. Campbell, J. H., Lengyel, J. A., and Langridge, J. (1973) *Proc. Natl. Acad. Sci. U.S.A.* **70,** 1841–1845

62. Hall, B. G. (1978) *Genetics* **90,** 673–681

63. Tipton, P. A., and Peisach, J. (1990) *Biochemistry* **29,** 1749–1756

64. Nemoz, G., Robert-Baudouy, J., and Stoeber, F. (1976) *J. Bacteriol.* **127,** 706–718

65. Kim, C., Song, S., and Park, C. (1997) *J. Bacteriol.* **179,** 7631–7637

66. Poulsen, T. S., Chang, Y. Y., and Hove-Jensen, B. (1999) *J. Bacteriol.* **181,** 7126–7130

67. Plumbridge, J., and Vimr, E. (1999) *J. Bacteriol.* **181,** 47–54

68. Stewart, V., and Yanofsky, C. (1985) *J. Bacteriol.* **164,** 731–740

69. Muse, W. B., and Bender, R. A. (1998) *J. Bacteriol.* **180,** 1166–1173

70. Zhou, L., Lei, X. H., Bochner, B. R., and Wanner, B. L. (2003) *J. Bacteriol.* **185,** 4956–4972

71. Lamark, T., Styrvold, O. B., and Strøm, A. R. (1992) *FEMS Microbiol. Lett.* **75,** 149–154

72. Eichhorn, E., van der Ploeg, J. R., Kertesz, M. A., and Leisinger, T. (1997) *J. Biol. Chem.* **272,** 23031–23036

73. van der Ploeg, J. R., Weiss, M. A., Saller, E., Nashimoto, H., Saito, N., Kertesz, M. A., and Leisinger, T. (1996) *J. Bacteriol.* **178,** 5438–5446

74. Iwanicka-Nowicka, R., and Hryniewicz, M. M. (1995) *Gene* **166,** 11–17

75. van der Ploeg, J. R., Eichhorn, E., and Leisinger, T. (2001) *Arch. Microbiol.* **176,** 1–8

76. van der Ploeg, J. R., Iwanicka-Nowicka, R., Bykowski, T., Hryniewicz, M. M., and Leisinger, T. (1999) *J. Biol. Chem.* **274,** 29358–29365